

# Oxidation behaviour of reaction-bonded alumina compacts using an $\text{Al}_{88}\text{Si}_{12}$ alloy precursor

S. H. YOKOTA, L. C. DE JONGHE

*Lawrence Berkeley Laboratory, Materials Sciences Division, University of California, Berkeley, CA 94720, USA*

M. N. RAHAMAN

*Department of Ceramic Engineering, University of Missouri-Rolla, Rolla, MO 65401, USA*

The oxidation behaviour of attrition-milled  $\text{Al}_{88}\text{Si}_{12}/\text{Al}_2\text{O}_3$  powder mixtures was investigated for the formation of mullite/ $\text{Al}_2\text{O}_3$  composites by the reaction bonded alumina (RBAO) process. Cylindrical powder compacts were heated at  $5^\circ\text{C min}^{-1}$  to temperatures between 450 and  $1400^\circ\text{C}$ . Oxidation occurred rapidly between ca. 400 and  $750^\circ\text{C}$ . Dense, outer reaction layers which formed at the lower temperatures inhibited complete oxidation and led to fracture of the body during continued heating to higher temperatures (above ca.  $850^\circ\text{C}$ ). While the incorporation of  $\text{ZrO}_2$  improved the oxidation of the samples, X-ray analysis indicated that the Si in the alloy reacted with the  $\text{ZrO}_2$  to form phases which prevented the formation of mullite at the temperatures used in the experiments.

## 1. Introduction

Reaction-formed or reaction-bonded materials are produced from a solid material which increases in mass during high temperature reaction with either a gas or a liquid. Reaction forming processes permit, in principle, near net-shape fabrication of bodies with complex shapes. Many applications, including those for alumina and alumina-based ceramics, require close dimensional tolerances [1]. Sintering shrinkages of 15% or more, which normally occur with conventional ceramic powder processing methods, make close control of the final dimensions of the body difficult. Furthermore, if the sintering process is not controlled properly, differential shrinkage can lead to warping. Thus, in many cases, expensive machining of the sintered body must be performed to achieve close dimensional control [2–4]. The machining step can also introduce critical surface flaws which reduce the fracture strength of the body. Near net-shape fabrication by reaction forming is therefore an attractive alternative to conventional ceramic powder processing methods.

Most studies of the reaction forming process have considered its application to Si-based ceramics, e.g.  $\text{Si}_3\text{N}_4$  and SiC. However, a number of recent studies have considered the application of the process to the fabrication of  $\text{Al}_2\text{O}_3$ -based materials [4–9]. The reaction-bonded alumina (RBAO) process described by Claussen et al. [4] involved vigorous milling of a mixture of Al metal and various ceramic oxide powders followed by sintering of the compacted powders under controlled conditions. With the RBAO technique, low-shrinkage ceramics were produced by countering the sintering shrinkage of the compact

with the volume expansion accompanying the oxidation of the metal phase. In theory, this process could be applied to any system in which the metal-to-oxide volume increase is at least equal to the pore volume in the green body. Wu and Claussen [10] used the RBAO process to fabricate mullite-based materials using Al, SiC and  $\text{Al}_2\text{O}_3$  as precursors. In this system, SiC was oxidized to  $\text{SiO}_2$  with the evolution of CO and  $\text{CO}_2$  gases. A 108% volume increase accompanied the formation of  $\text{SiO}_2$  and its subsequent reaction to form mullite. The large volume change, combined with the shrinkage during heating, produced an overall shrinkage 0.1% and a final density of 93% of the theoretical value.

The formation of mullite-based ceramics by incorporation of Si into  $\text{Al}_2\text{O}_3$ -based starting materials by the RBAO process could be achieved through the use of the precursors other than SiC. The purpose of this research was to investigate the feasibility of producing low-shrinkage mullite/alumina composites by the RBAO process through the use of mixtures of  $\text{Al}_{88}\text{Si}_{12}$  and  $\text{Al}_2\text{O}_3$  powders. For this system, the volume increase, relative to the volume of the reactants, arising from the oxidation reaction to form mullite and alumina is calculated to be ca. 45%. The melting point of the alloy,  $577^\circ\text{C}$ , is well below the sintering temperature of the  $\text{Al}_2\text{O}_3$  powder. Microstructural and compositional changes during controlled heat treatment of the compacted powders were studied.

## 2. Experimental procedure

The  $\text{Al}_{88}\text{Si}_{12}$  (Johnson Matthey, MA) and  $\text{Al}_2\text{O}_3$  (38 Alundum grade, Norton Co., MA) powders were used

as-received from the manufacturers. The  $\text{Al}_{88}\text{Si}_{12}$  powder consisted of globular particles with a diameter of  $< 40\ \mu\text{m}$  while the  $\text{Al}_2\text{O}_3$  powder consisted of angular particles with an average size of ca.  $15\ \mu\text{m}$ . The coarse, angular nature of the  $\text{Al}_2\text{O}_3$  particles was found to be beneficial for the milling process; finer or globular powder caused welding and agglomeration of the metal particles. For most of the experiments, the starting composition of the mixture was 50 vol%  $\text{Al}_{88}\text{Si}_{12}$  and 50 vol%  $\text{Al}_2\text{O}_3$ . In a few experiments,  $\text{ZrO}_2$  powder stabilized with ca. 8 mol %  $\text{Y}_2\text{O}_3$  (SC87; Magnesium Electron Inc., NJ) was added to produce a starting composition of 50 vol %  $\text{Al}_{88}\text{Si}_{12}$ , 40 vol %  $\text{Al}_2\text{O}_3$  and 10 vol %  $\text{ZrO}_2$ . The  $\text{ZrO}_2$  powder served to improve the oxygen transport through the mixture during the reaction. No binder was needed to achieve good compaction of the mixture but 1 wt % dispersant (Daxad 34; W.R. Grace & Co., MA) was added to reduce agglomeration during milling.

The powder mixture was dispersed in reagent grade isopropanol and milled for 7 h in a batch attritor mill (Model HD-01, Union Process, OH) using high-purity  $\text{ZrO}_2$  balls as the milling media. The shaft speed of the mill was set at 600–650 rpm (the maximum speed for the instrument) and the milling was performed in a closed container to prevent evaporation of the isopropanol and excessive oxidation of the metal particles. After milling, the  $\text{ZrO}_2$  balls were removed and the slurry was dried at room temperature. The dried mixture was then lightly ground in a mortar and pestle and dried overnight in air at  $100^\circ\text{C}$  to remove any remaining solvent. In one set of experiments precautions were taken to minimize exposure of the mixture to an oxidizing environment. The powder mixture was dispersed in anhydrous isopropanol and, following milling, rotovap drying and vacuum drying were used to evaporate the solvent.

The dried powder was pressed in a stainless steel die under a pressure of ca. 50 MPa to form cylindrical pellets (6 mm in diameter and ca. 6 mm in length). The pellets were then compacted further by cold isostatically pressing (CIP) at 400–700 MPa to produce samples with green densities of 66–73% of the theoretical value. Firing was performed in air in a horizontal tube furnace at a heating rate of  $5^\circ\text{C}\ \text{min}^{-1}$ ; the samples were held for fixed times (5–420 min) at temperatures between 450 and  $1500^\circ\text{C}$ , and then cooled to room temperature by switching off the furnace power.

Samples for microscopy were prepared by slicing the fired pellets in a plane perpendicular to the axial direction, followed by polishing. Optical microscopy and scanning electron microscopy (SEM) were used to observe the well-defined, concentric reaction layers which formed during firing. Compositional variation across the samples was analysed by energy dispersive spectroscopy (EDS) in the SEM. Etched samples were also used in a few observations. The etching conditions were either 5 min in 0.1 M HF solution at room temperature or 10 min in 7 M NaOH solution at  $50^\circ\text{C}$ . X-ray diffraction (XRD) was carried out on polished surfaces or on powder. Fragments from selected regions of the fired body were ground to produce the powder.

The reaction products in the present study were insulating oxides, but the unreacted  $\text{Al}_{88}\text{Si}_{12}$  alloy was a good conductor. Information on the state of passivation of the alloy produced by surface oxidation and the distribution of the alloy in the sample could be obtained from electrical conductivity measurements. In the investigations, two-point resistivity measurements were made across different regions of the polished samples (Fluke 77 Multimeter).

### 3. Results and discussion

The results for the microstructure, composition and electrical resistivity of the powder compacts which were reacted under controlled heating conditions are described in the following sections.

#### 3.1. Microstructure of the reaction bonded materials

All the samples heated above the melting temperature of the  $\text{Al}_{88}\text{Si}_{12}$  alloy ( $577^\circ\text{C}$ ) formed well-defined reaction rings which were concentric with the axis of the powder compact. Fig. 1a–d shows photographs of the polished surfaces of samples which were cold isostatically pressed under a pressure of 400 MPa (giving a green density of ca. 0.66%) and fired under various temperature schedules. A different set of green bodies was used for each heating schedule. Fig. 1a shows a sample fired at  $550^\circ\text{C}$  for 6 h; a thin reaction ring around the circumference of the sample is barely detectable. The sample shown in Fig. 1b was fired at  $550^\circ\text{C}$  for 6 h, and then at  $850^\circ\text{C}$  for another 6 h; a small radial crack can be seen terminating near the core-reaction ring interface. It was found that almost all of the samples fired for more than 3 h at  $850^\circ\text{C}$  contained cracks. Experiments performed in a dilatometer revealed that the cracks occurred during the isothermal hold at  $850^\circ\text{C}$  and not during the cooling stage. Fig. 1c shows a sample which was heated directly to  $850^\circ\text{C}$  (i.e. without any hold at lower temperature) and held for 3 h; extensive radial cracks are easily observed in the outer reacted layer. It can be seen from Fig. 1b and c that the sample heated directly to  $850^\circ\text{C}$  had a more sharply defined reaction ring and more extensive cracking than the sample which was held at  $550^\circ\text{C}$  prior to heating to  $850^\circ\text{C}$ . For the sample heated directly to  $850^\circ\text{C}$ , holding for longer times (e.g. ca. 7 h) resulted in fragmentation. Fig. 1d shows a sample which was heated according to the schedule described for Fig. 1b and then heated for 3 h at  $1400^\circ\text{C}$ . The reaction layer nearest to the surface of the sample is white, suggesting that complete oxidation of the metal phase occurred. However, a partly reacted core remains.

Fig. 1b and c show that the radial cracks run through the reaction ring and terminate at, or are deflected by, the interface between the reacted ring and the unreacted core. The radial nature of the cracks indicates that they were produced during an isothermal heat treatment ( $850^\circ\text{C}$ ), they cannot be explained in terms of a mismatch in thermal expansion. Sintering of the reacted ring, which is constrained by a

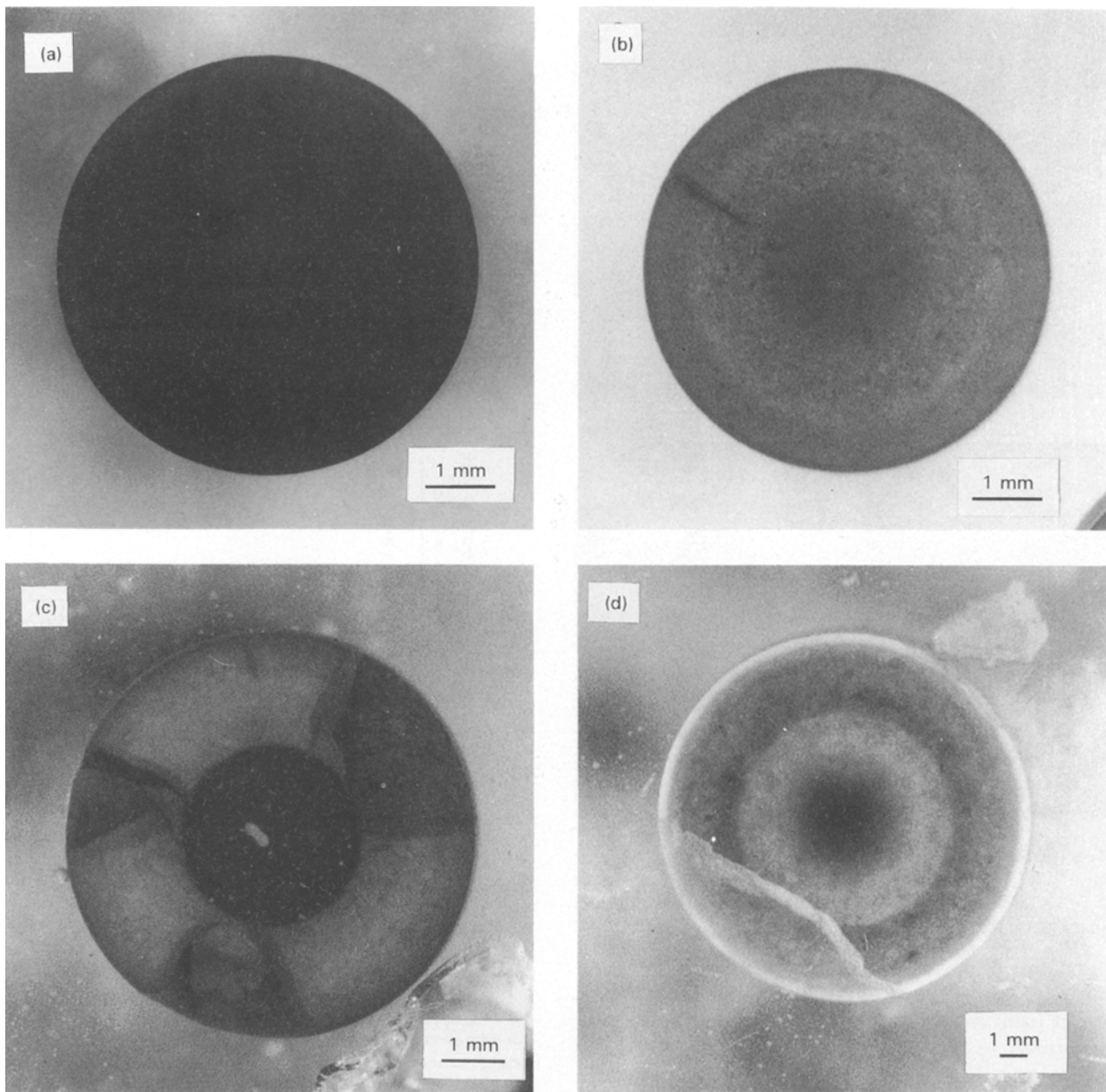


Figure 1 Optical micrographs of the polished surfaces of  $\text{Al}_{88}\text{Si}_{12}/\text{Al}_2\text{O}_3$  powder compacts after heating (a) for 6 h at  $550^\circ\text{C}$ , (b) for 6 h at  $550^\circ\text{C}$  followed by 6 h at  $850^\circ\text{C}$ , (c) for 3 h at  $850^\circ\text{C}$  and (d)  $1400^\circ\text{C}$ .

non-shrinking core, is also an unlikely source of the cracking. This mechanism would be active during heat-up or early in the isothermal heat treatment; as outlined earlier, the cracking occurred after the sample was held for ca. 3 h at  $850^\circ\text{C}$ . The reaction process must therefore be the source of the cracking.

Solid-gas reaction in a porous compact has been modelled by Szekely *et al.* [12]. They proposed that the gas in the pores (e.g.  $\text{O}_2$ ) was rapidly consumed during the early stages of the heat treatment and any further diffusion of gas into the sample was limited by the reacted surface layer. In the present experiments, an oxidized reaction ring would be expected to form during heat-up. When the  $\text{Al}_{88}\text{Si}_{12}$  alloy melting temperature ( $577^\circ\text{C}$ ) was reached, therefore, the compact was encased in a highly-oxidized reaction ring. However, except for a thin passivation layer, the core of the compact was unreacted. If the passivation layer can be easily disrupted, then the alloy in the core can melt and flow into the pores of the core and the oxidized

reaction ring, thereby closing the high diffusivity paths for oxygen. Further oxidation then takes place through much slower ionic transport mechanisms, such as oxygen diffusion through the grain boundaries or cation diffusion through the reaction ring. The volume expansion accompanying the core oxidation then creates tensile stresses in the reaction ring which can lead to cracking.

Fig. 2a and b shows the differences in microstructure between the reaction ring and the core for samples heated at  $5^\circ\text{C min}^{-1}$  to  $600^\circ\text{C}$  and held at this temperature for 5 min. The core is seen to be denser than the reaction ring. As outlined earlier, the melting and flow of the alloy in the core can lead to closure of the high diffusivity paths for oxygen. Thus, further oxidation of the core is severely inhibited. However, an interfacial phase between the reaction ring and the core, which acts as a diffusion barrier, can also account for this difference between the reaction ring and the core. For example, a dense, glassy interfacial layer

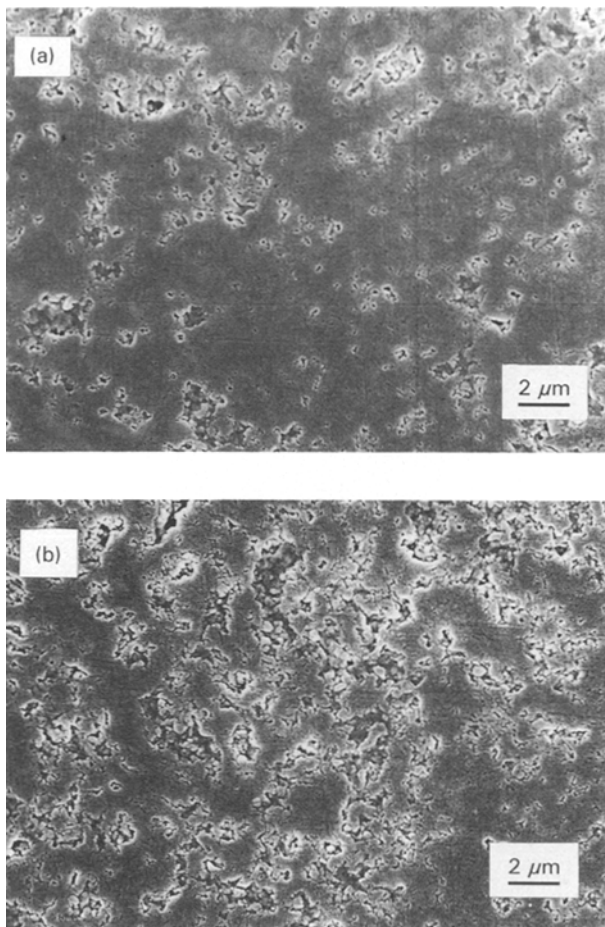


Figure 2 Scanning electron micrographs of the polished surface of an  $\text{Al}_{88}\text{Si}_{12}/\text{Al}_2\text{O}_3$  powder compact which was heated for 5 min at  $600^\circ\text{C}$  showing the difference in density between (a) the unreacted core and (b) the reaction ring.

can act as a barrier for diffusion of aluminium ions at lower temperatures or for oxygen ions at higher temperatures. In the directed melt oxidation (DIMOX) process, a thin interfacial phase of  $\text{MgAl}_2\text{O}_4$  has been observed between the melt and a surface layer of  $\text{MgO}$ . The  $\text{MgO}-\text{MgAl}_2\text{O}_4$  double layer causes the originally silvery surface of the melt to appear dark grey [6, 13]. A small amount of Si found in the  $\text{MgAl}_2\text{O}_4$  layer may help to decrease the activity of the Mg (possibly through the formation of  $\text{Mg}_2\text{Si}$ ), thus preventing the recombination of  $\text{Mg}^{2+}$  and  $\text{O}^{2-}$  on the underside of the  $\text{MgO}$  layer [6]. In the DIMOX process, the interfacial layer of  $\text{MgAl}_2\text{O}_4$  does not appear to hinder ionic diffusion. However, the presence of Si in both the DIMOX process and the current work requires further investigation to determine the significance of an interfacial phase.

Fig. 3a–c shows data for the furnace temperature, fractional weight change and reaction ring thickness during a typical heat treatment of  $\text{Al}_{88}\text{Si}_{12}/\text{Al}_2\text{O}_3$  powder compacts (green density ca. 0.66) which were cold isostatically pressed at 400 MPa. A different sample was used for each run to a given temperature. The weight change was seen to increase rapidly and reached a value of ca. 16% at the end of the first heat-up stage (ca.  $850^\circ\text{C}$ ). However, there was only a small increase in weight during holding at  $850^\circ\text{C}$  or further heating to  $1400^\circ\text{C}$ . The total weight change at the end

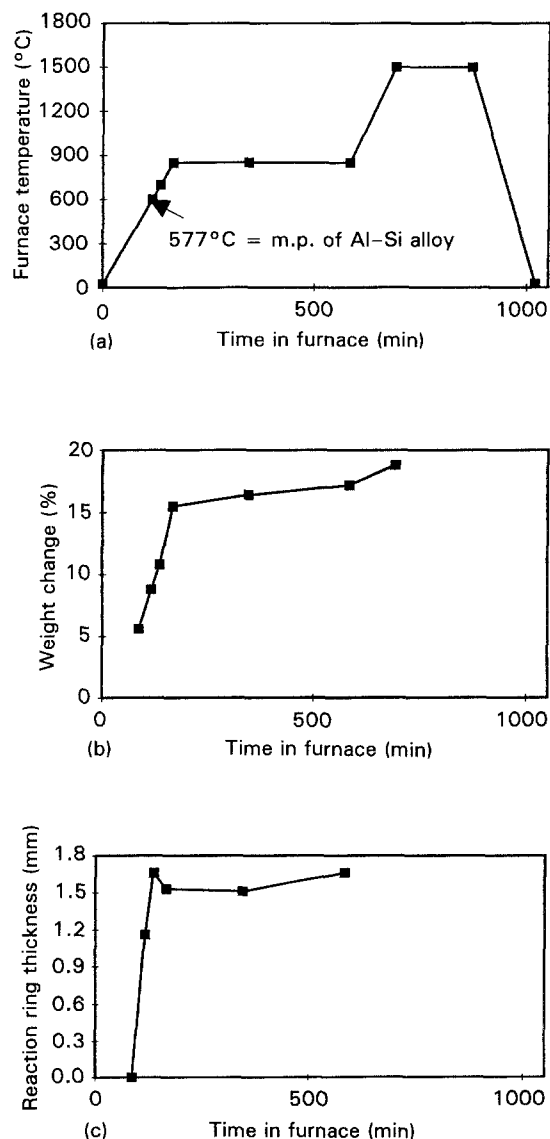


Figure 3 Data for (a) the temperature schedule of the reaction bonding process and the corresponding values for (b) the fractional weight change and (c) the thickness of the reaction ring for powder compacts heated to various temperatures.

of the experiment was ca. 19%, corresponding to 60% of the theoretical value for the fully reacted material. The formation of a reaction ring was detectable at ca.  $400^\circ\text{C}$  and its thickness increased rapidly with temperature up to ca.  $700^\circ\text{C}$ , after which there was almost no further increase. The weight change and reaction ring thickness data indicate that the major part of the oxidation took place between ca. 400 and  $700^\circ\text{C}$ . The data for the fractional weight change, reaction ring thickness and linear shrinkage of the sample during the first heat-up stage to  $850^\circ\text{C}$  are shown in more detail in Fig. 4a–c. The sample shrunk slightly, with the shrinkage reaching a maximum value of ca. 0.5% at  $700^\circ\text{C}$ , after which it decreased to almost zero at ca.  $850^\circ\text{C}$ . Heating above  $850^\circ\text{C}$  or for longer times at this temperature lead to an expansion of the sample which created tensile stresses in the reaction ring and, ultimately, cracking.

For identical heat treatments, the reaction layer was thinner for samples with higher green density, suggesting that lower porosity reduced oxygen diffusion into the compact. A similar observation was made by Wu

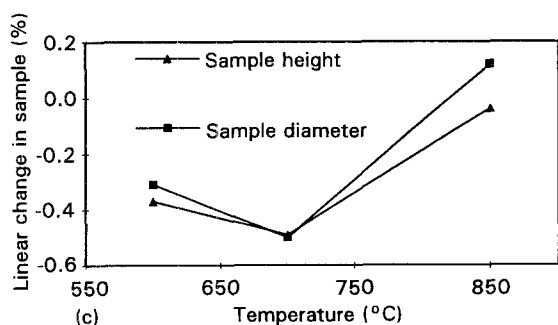
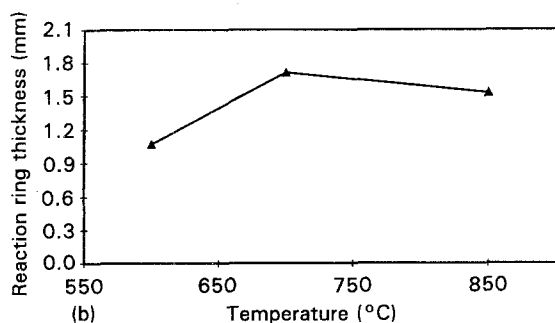
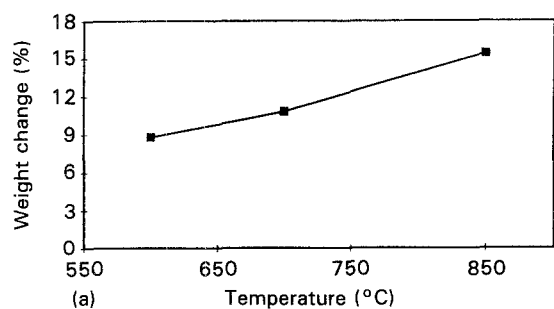


Figure 4 Data for (a) the fractional weight change, (b) the reaction ring thickness and (c) the fractional change in dimension of powder compacts heated to temperatures between 600 and 850°C.

*et al.* [11], who calculated that the mean free path of  $O_2$  at 700°C was 6–7 times larger than the average pore radius in compacts of 1  $\mu\text{m}$  powder formed by cold-isostatic pressing between 300 and 900 MPa. In the present work, the incorporation of  $ZrO_2$  powder (10 vol %) into the  $Al_{88}Si_{12}/Al_2O_3$  mixture produced an increase in the fractional weight change of the sample under identical heat treatment. The  $ZrO_2$  phase provided a high diffusivity path for oxygen, compared to the reacted material. However, as outlined later, the reaction between  $ZrO_2$  and Si led to the formation of zirconium silicate phases which hindered the formation of mullite.

### 3.2. Chemical composition

EDS analysis showed that, prior to milling, the powder mixtures had a composition of 93 at % Al and 7 at % Si. After milling, the powder composition was 90 at % Al, 6 at % Si and 4 at % Zr. The Zr fraction is attributed to wear of the  $ZrO_2$  grinding media used to comminute the powder mixture. Assuming that the reaction involved no loss or redistribution of the phases in the powder compact, then the atomic concentrations of the metals should not change. Table I

TABLE I Composition of the reaction bonded powder mixtures

Sample	At % Al	At % Si	At % Zr
Unfired	90	6	4
850°C, ring 5 min, core	88	6	5
850°C, ring 3 h, core	90	5	5
1500°C, ring 1 h, core	87	9	4
	91	4	5
	87	9	4

shows the atomic concentrations of Al, Si and Zr for the milled powder mixture and for the reaction bonded powder compacts after known heating schedules.

The data in Table I indicate that the Zr concentration remained essentially constant, but there small differences occurred in the Si and Al concentrations. In the unreacted core, while the Si concentration was slightly higher than the value for the unfired sample, the Si and Al concentrations were approximately independent of the heating schedules. For the reaction ring, the Al concentration increased slightly and the Si concentration decreased slightly with longer heating times or with higher temperatures; the Al/Si ratio therefore increased significantly with longer heating times or at higher temperatures. The factors which can produce these observed changes in the composition of the core should be considered.

As outlined earlier, at temperatures above its melting point, the  $Al_{88}Si_{12}$  alloy in the unreacted core may melt and flow into the outer reaction ring. Since the Si concentration in the alloy is higher than in the  $Al_{88}Si_{12}/Al_2O_3$  powder mixture, a decrease in the Si concentration in the core would be expected. Therefore, the transport of the alloy into the reaction ring cannot, by itself, account for the observed difference in composition of the core. Another process which can lead to compositional changes is the preferential oxidation of the Al in the  $Al_{88}Si_{12}$  alloy. Wagner [15, 16] has shown that during the oxidation of alloys, segregation of the preferentially oxidized element to the surface occurs; the reaction layer would then further retard oxidation of the slower reacting metal. In present system, the oxidation rate of the Al is expected to be faster than that for the Si. At any interface between the reaction ring and the unreacted core, oxidation leads to a reacted layer that is richer in Al. Over the course of the heat treatment, a reaction ring with a higher Al/Si ratio and an unreacted core with a lower Al/Si ratio would be expected to be formed. However, this process appears unlikely because it would involve significant diffusion of matter over relatively large distances.

Observation of the polished cross-sections of the reaction-bonded material in the SEM showed that the core has a composite microstructure. Fig. 5 shows a micrograph of the core of the sample heated to 1400°C (see Fig. 1d for a micrograph of the entire cross-section). The light-coloured inclusion phase with a predominantly elongated morphology has a Si/Zr atomic ratio of ca. 1, as measured by EDX analysis.

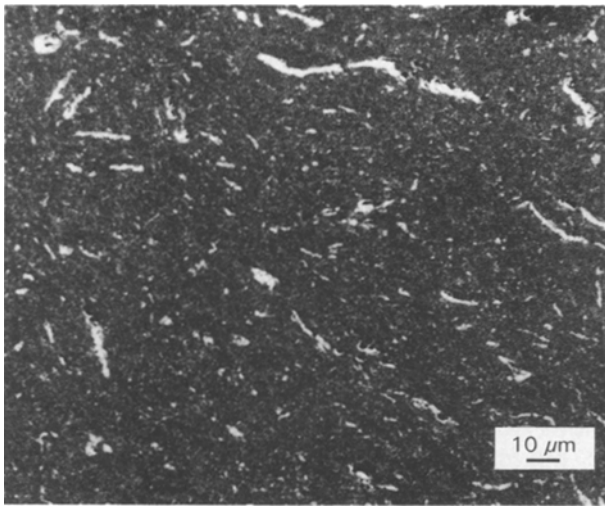


Figure 5 Scanning electron micrograph of the polished surface of a powder compact which was heated to 1400 °C, showing ZrSiO<sub>4</sub> inclusions in the core of the sample.

This atomic ratio corresponds to the composition of zircon, ZrSi<sub>4</sub>, which was detected by XRD. The darker matrix phase had a composition of ca. 93 at % Al, 5.5 at % Si and 1.5 at % Zr. The relatively high concentration of Si in the ZrSiO<sub>4</sub> inclusion phase may have distorted the Si signal and contributed to the apparent high concentration of Si in the core. Samples treated at lower temperatures contained inclusions with different Si/Zr atomic ratios. For example, the core of the sample which was heated to 550 °C (Fig. 1a) contained inclusions with a Si/Zr atomic ratio of ca. 2. XRD analysis showed, in addition, the presence of a small amount of ZrSi<sub>2</sub> in the sample.

The presence of ZrSi<sub>2</sub> and ZrSiO<sub>4</sub> during the reaction bonding process would preclude the formation of aluminosilicate compounds at the temperatures used in these experiments (up to 1400 °C). ZrSi<sub>2</sub> is stable up to ca. 1420 °C and ZrSiO<sub>4</sub> is stable even above ca. 1500 °C. The reaction hot-pressing of ZrSiO<sub>4</sub>/Al<sub>2</sub>O<sub>3</sub> mixtures at 1450 °C has been investigated by di Rupo *et al.* [18], who showed that the reaction process occurred concurrently with densification. Therefore, the data of di Rupo *et al.* [18] indicate that the formation of aluminosilicate compounds in the present work would require sintering temperatures where appreciable densification occurs. The lower driving force for densification during sintering would require temperatures above ca. 1500 °C to obtain a dense ceramic.

### 3.3. Resistivity of the samples

The green compacts, samples heated below ca. 500 °C and samples heated above ca. 850 °C were found to be electrically insulating. However, the electrical resistivity of the core and the reaction ring in the samples heated to temperatures between 600 and 850 °C was relatively small; the results for these samples are shown in Fig. 6. The results indicate that the milling process formed a passivation layer on the Al<sub>88</sub>Si<sub>12</sub> particles, and heat treatment above 850 °C was sufficient to produce highly oxidized layers on the alloy

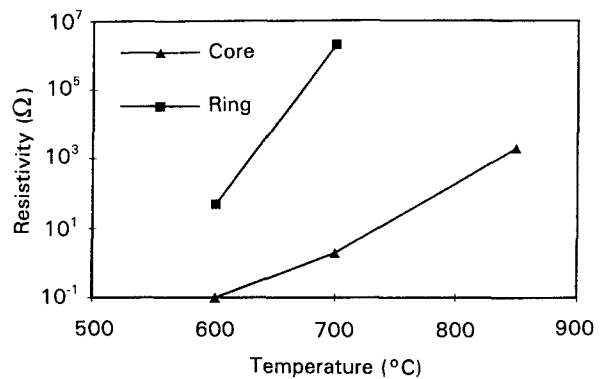


Figure 6 Electrical resistivity of the reaction ring and the core for powder compacts that were reaction bonded at temperatures between 600 and 850 °C.

particles. However, the low resistivity of the samples at ca. 600 °C (i.e. above the melting point of the alloy) show that the passivation layer formed during milling and heat-up was insufficient to contain the melted alloy; flow of the melt occurred not only in the core of the sample but also into the interconnected porosity of the reaction ring. The increase in resistivity at higher temperatures (e.g. 700 °C) reflected the oxidation of the melted alloy. The resistivity of the reaction ring was much higher than that of the core because of the higher oxidation rate of the ring.

## 4. Conclusions

The reaction bonding of Al<sub>88</sub>Si<sub>12</sub>/Al<sub>2</sub>O<sub>3</sub> powder mixtures for the formation of mullite/alumina bodies was investigated during heating at a fixed rate (5 °C min<sup>-1</sup>) to temperatures up to 1400 °C. The main part of the oxidation process occurred between ca. 400 and 800 °C. The fired samples had a structure consisting of a highly oxidized reaction ring and a relatively unreacted core.

Microstructural observations and electrical resistivity measurements indicated that, above its melting point, the Al<sub>88</sub>Si<sub>12</sub> alloy in the unreacted core melted and flowed into the pores of the core and the reaction ring. The expansion accompanying subsequent oxidation of the melt generated tensile stresses and radial cracking in the reaction ring. The attainment of a dense, fully reacted body by the reaction bonding process required elimination of appreciable melt flow and the preservation of interconnected porosity until the later stages of the heating process.

The incorporation of ZrO<sub>2</sub> into the mixture during the milling step or through deliberate additions improved the oxidation process but led to the formation of relatively stable compounds of Zr and Si. These compounds precluded the formation of mullite at the temperatures used in the experiments.

## Acknowledgement

This work was supported by the Division of Materials Science, Office of Basic Energy Research, US Department of Energy, under contract No.

## References

1. G. MACZURA, K. J. MOODY and E. M. ANDERSON, *Ceram. Bull.* **71** (1992) 780.
2. W. D. KINGERY, H. K. BOWEN and D. R. UHLMANN, in "Introduction to ceramics", 2nd Edn (John Wiley & Sons, New York, 1976) p. 508.
3. M. E. WASHBURN and W. S. COBLENTZ, *Ceram. Bull.* **67** (1988) 356.
4. N. CLAUSSEN, N. A. TRAVITZKY and S. WU, *Ceram. Engng. Sci. Proc.* **11** (1990) 806.
5. M. NEWKIRK, A. W. URQUHART, H. R. ZWICKER and E. BREVAL, *J. Mater. Res.* **1** (1986) 81.
6. O. SALAS, H. NI, V. JAYARAM, K. C. KLACH, C. G. LEVI and R. MEHRABIAN, *J. Mater. Res.* **6** (1991) 1964.
7. B. R. MARPLE and D. J. GREEN, *J. Amer. Ceram. Soc.* **71** (1988) C471.
8. M. D. SACKS, N. BOZKURT and G. W. SCHEIFFLE, *J. Amer. Ceram. Soc.* **74** (1991) 2428.
9. J. M. WU and C. M. LIN, *J. Mater. Sci.* **26** (1991) 4631.
10. S. WU and N. CLAUSSEN, *J. Amer. Ceram. Soc.* **74** (1991) 2460.
11. S. WU, D. HOLZ and N. CLAUSSEN, *J. Amer. Ceram. Soc.* **76** (1993) 970.
12. J. SZEKELY, J. W. EVANS and H. Y. SOHN, in "Gas-solid reactions" (Academic Press, New York, 1976) p. 130.
13. S. ANTOLIN, A. S. NAGELBERG and D. K. CREBER, *J. Amer. Ceram. Soc.* **75** (1992) 447.
14. M. SINDEL, N. A. TRAVITZKY and N. CLAUSSEN, *J. Amer. Ceram. Soc.* **73** (1990) 2615.
15. C. WAGNER, *J. Electrochem. Soc.* **103** (1956) 627.
16. C. WAGNER, *J. Electrochem. Soc.* **99** (1952) 369.
17. R. MOLINS, J. D. BARTOUT and Y. BIENVENU, *Mater. Sci. Engng.* **A135** (1991) 111.
18. E. DI RUPO, E. GILBART, T. G. CARRUTHERS and R. J. BROOK, *J. Mater. Sci.* **14** (1979) 705.

Received 5 April 1993

and accepted 16 February 1994